

Surface morphology of biofouling in membrane bioreactor treating actual sewage

Aida Isma M. I.^{1*}, Munira Mohammad¹, Putri Razreena Abdul Razak², Hazmin Mansor³,
A. Idris⁴, Siti Baizura M.⁴

¹ Centre for Water Research, Faculty of Engineering, Built Environment & Information Technology, SEGi University, Kota Damansara, 47810, Petaling Jaya, Selangor Darul Ehsan, Malaysia

² SIRIM Berhad, Persiaran Dato' Menteri, P.O.Box 7035, 40700 Shah Alam, Selangor Darul Ehsan, Malaysia

³ Department of Engineering, Faculty of Engineering and Life Sciences, Universiti Selangor, Jalan Timur Tambahan, 45600 Bestari Jaya, Selangor Darul Ehsan, Malaysia

⁴ Department of Chemical and Environmental Engineering, Faculty of Engineering, Universiti Putra Malaysia, 43400 Serdang, Selangor Darul Ehsan, Malaysia

Received: May 10, 2022; **Accepted:** June 2, 2022; **Published online:** August 30, 2022

Abstract: Biofouling is the most challenging operational problem in membrane bioreactors. The goal of this study is to evaluate the foulants mechanism by profiling the foulants morphology in a membrane bioreactor treating actual sewage. A 10 m² hollow fiber membrane was set up at MLSS of 9 g/L and HRT of 8 hours. CLSM and FESEM were used to characterize the membrane morphologies. The trans-membrane pressure was monitored, and membrane samples were analysed on weekly basis. The performance of the membrane bioreactor treating the actual sewage showed a remarkable result. The biofilm and cake layer formation dominated the majority of fouling in the MBR operation, resulting in slower permeation flux decay over time. The evaluation of fouling layers and the mechanism of biofouling development through profiling of foulant morphology using FESEM and CLSM revealed that the membrane experienced mild internal pore-clogging, implying that fouling occurred mainly on the membrane surface. The fluorescent staining of CLSM images revealed that proteins, α -D-glucopyranose polysaccharides, and lipids were aggregated into clusters with protein depth thickness recorded at 22 μ m. FESEM images revealed that the membrane experienced mild internal pore-clogging and had marginally reduced the overall water permeability and severely reduced the mass transfer coefficient. It can be concluded that proteins and microbial cells were

*e-mail: aidaisma@segi.edu.my

the primary constituents of the fouling layer which may have contributed to the membrane performance deterioration after fouling.

Keywords: Biofouling, CLSM, FESEM, Morphology, Sewage

1 Introduction

Membrane biofouling has attracted much attention in recent years as it hinders the application and development of membrane bioreactors (MBRs) (Yang et al., 2020). Biofouling is the most challenging operational problem in membrane bioreactors which reduces flux and increases the pressure drop across the membrane causing membrane failure which greatly compromises the efficiency of the treatment processes. Wastewater characteristics, such as particle size, viscosity, floc structure, extra polymeric substances, soluble microbial products, and the organic loading rate, influence and alter microbial behavior as well as the biofilm character on the membrane surface, all of which could have an impact on membrane biofouling (Alrhoun et al., 2014).

Several studies have been conducted to better understand how to predict membrane fouling. These studies should concentrate on membrane flux, trans-membrane pressure, and other operating conditions (Hu et al., 2016). A multi-step estimation of the permeability rate may be more cost-effective when evaluating fouling in wastewater treatment. The interfacial interactions in membrane bioreactors determine adhesion and fouling caused by pollution.

As a result, the morphology of foulants and the bound extra polymeric substances secreted by microbes are important properties to investigate. The way forward will be to predict membrane flux and recovery for the specific MBR operation treating wastewater. Foulant reduction prevents internal scaling and biofouling overgrowth while increasing membrane permeability, resulting in improved bioreactor performance. The goal of this study is to evaluate the foulants mechanism by profiling the foulants morphology in a membrane bioreactor treating actual sewage.

2 Materials and Methods

2.1. Membrane bioreactor set-up and start-up

Figure 1 shows the schematic diagram of the membrane bioreactor configuration used in this study. An 80-liter bioreactor is filled with a hollow fiber PVDF membrane with a surface area of 10 m². This MBR was set up at mixed liquor suspended solids (MLSS) of 9 g/L and a hydraulic retention time of 8 hours. The dissolved oxygen was kept above the critical level of 2 mg/L. The MBR was activated and allowed to acclimate for two weeks with actual sewage. This study was conducted at a local wastewater treatment plant in Kuala Lumpur. Samples of the membrane were taken from the bioreactor for further analysis. The MBR operation was monitored twice a week and was turned off when the trans-membrane pressure exceeded 500 mmHg.

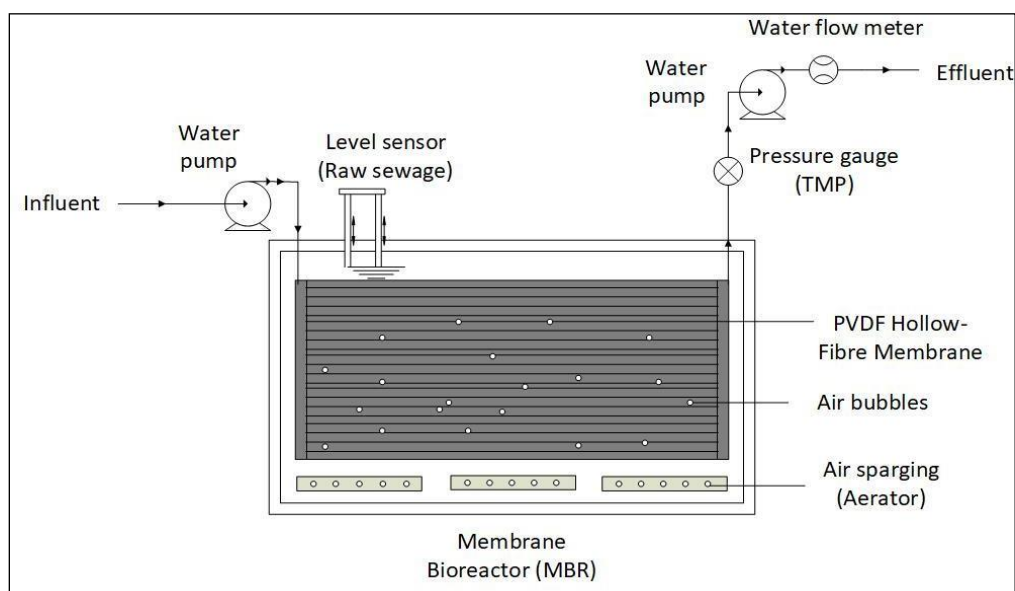


Figure 1: Schematic diagram of the MBR configuration in this study.

2. 2. Chemical structure characterization of biofouling layer: FESEM-EDX analysis

Membranes with biofilm were removed from the membrane bioreactor at various times of operation. All samples were dried for 24 hours at 105 °C. The sample was coated with a gold sputter prior to the FESEM analysis (Hitachi SU8220). The elements in the cake layer were identified by using the energy dispersive X-ray (NOVA NanoSEM 230, USA).

2. 3. Staining and imaging

The foulants were stained with the following reagents: FITC, Con A conjugated with tetramethylrhodamine, SYTO 63 (Sigma Aldrich), Nile red, and calcofluor white. These reagents were produced following the method outlined by Yang et al. (Yang et al., 2007). Internal fouling layer structure was studied using confocal laser scanning microscopy (CLSM; Leica TCS SP8 Confocal Spectral Microscope Imaging System, Germany). 10x or 20x objective images were analysed with Leica confocal software. SYTO 63 fluorescence was measured at 633 nm and 650–760 nm (red). Con A conjugates were detected at 543 and 550–590 nm (light blue). Nile Red emission wavelengths ranged from 630 to 700 nm (yellow). FITC was detected using 488 nm excitation and 500–540 nm emission (green). SYTOX Blue fluorescence intensity was measured at 458 nm excitation and 460–500 nm emission (purple). Excitation at 405 nm and emission widths of 410–480 nm was used to measure the fluorescence of calcofluor white (blue). At 5 µm above the membrane surface, the pictures were scanned at a resolution of 100 µm x 100 µm.

2. 4. Wastewater quality analysis

The typical parameters of effluent were determined according to APHA Standard Methods for Examination of Water and Wastewater (APHA, 2005).

3 Results and Discussions

Table 1 shows the effluent quality recorded during the study. All effluent parameters comply with the effluent discharge standards of Malaysia. However, it should be noted that the ammoniacal nitrogen ($\text{NH}_3\text{-N}$) removal might attribute to the simultaneous nitrification/denitrification (SND) processes (Adoonsook et al., 2019).

Table 1. Effluent quality of the membrane bioreactor in this study.

Parameter	Effluent (mg/L)
Chemical oxygen demand (COD)	78.0 ± 37.15
Biological oxygen demand (BOD_5)	15.7 ± 13.08
Total suspended solids (TSS)	29.5 ± 19.96
Ammoniacal nitrogen ($\text{NH}_3\text{-N}$)	8.3 ± 10.21
Phosphorus (PO_4^{3-})	5.4 ± 6.05

3. 1. Biofouling in membrane bioreactor

Throughout the assessment period, the experimental MBR pilot plant was continuously run on-site, using actual sewage as a source of feed wastewater. The PVDF hollow membrane was immersed in the center compartment of the MBR with an initial MLSS concentration of approximately 9 g/L. Figure 2 depicts the evolution of foulant in relation to TMP readings recorded over time. On day 0, the TMP reading for the newly installed membrane was approximately 200 mmHg. The first increase in TMP was recorded from 200 mmHg to 300 mmHg and was possibly caused by bacterial adsorption and metabolite binding on the membrane surface, which caused the pore blocking phenomenon. The foulants slowly seeped through the intrinsic pores at the membrane surface, as revealed by FESEM images (Image 1). The Phase 2 observation discovered that the biofouling layer grew on the membrane surface over time, followed by the formation of a dense and thick layer of foulant. This condition could be influenced by an accumulation of microbial communities that have adapted and colonized in the MBR (Image 2), resulting in a rise in TMP from 300 mmHg to 400 mmHg. Agglomerations of extracellular polymeric substances excreted by microbes had adhesive properties, were semi-attached to the bacteria cells, and disperse out from the bacteria cells in large clusters (Isik et al., 2020). In phase 3, the biofilm expanded across the membrane surface area, and the cake layer compacted (Image 3), reducing membrane porosity. In this condition, higher pressure was required to operate, resulting in a rapid increase in the TMP reading, which reached more than 500 mmHg. The presence of a cake layer increased the roughness of the membrane surface as well as the presence of peaks and fissures, resulting in the entrapment of various foulants on the surface. The fouling layer had grown to a thickness of 693 μm (Image 4).

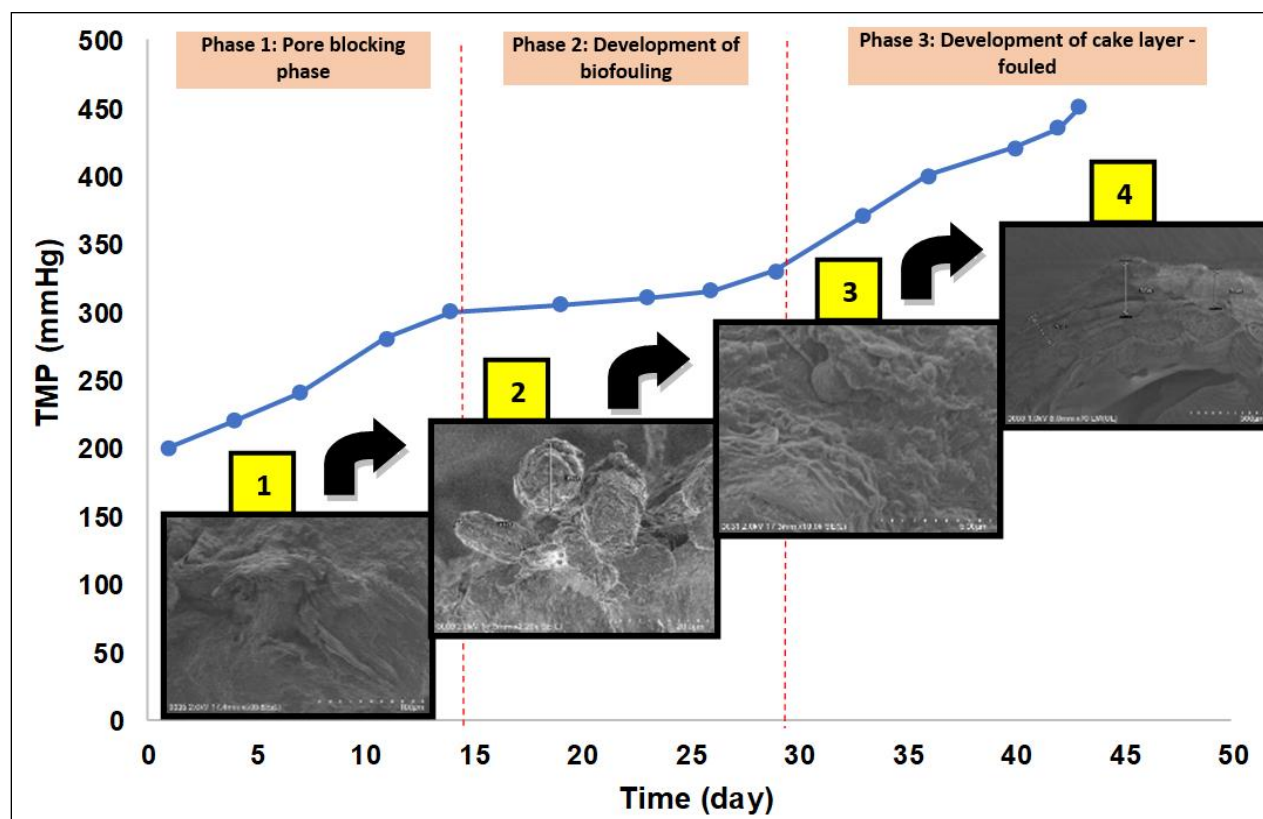


Figure 2: Biofouling development in this study.

3. 2. Confocal laser scanning microscopy

The accumulation of bacterial clusters increases fouling resistance (Isik et al., 2020) and the correlation to in situ microorganisms and their three-dimensional environments, such as in food matrixes, biofilms, and the gut can be captured using a confocal laser scanning microscope (Canette and Briandet, 2014). The CLSM images of the foulants layer deposited on the membrane surface are shown in Figure 3. According to the findings, the developed biofouling layer was primarily composed of protein, which is abundant in sewage. Polysaccharides, lipids, and microorganisms are among other biological components discovered. These biopolymers will then adhere to the bacterial cells in a real-time organic membrane fouling formation, which are similar to findings conducted by Fortunato et al. (Fortunato et al., 2019) and Du et al. (Du et al., 2020) after being absorbed through the membrane pores.

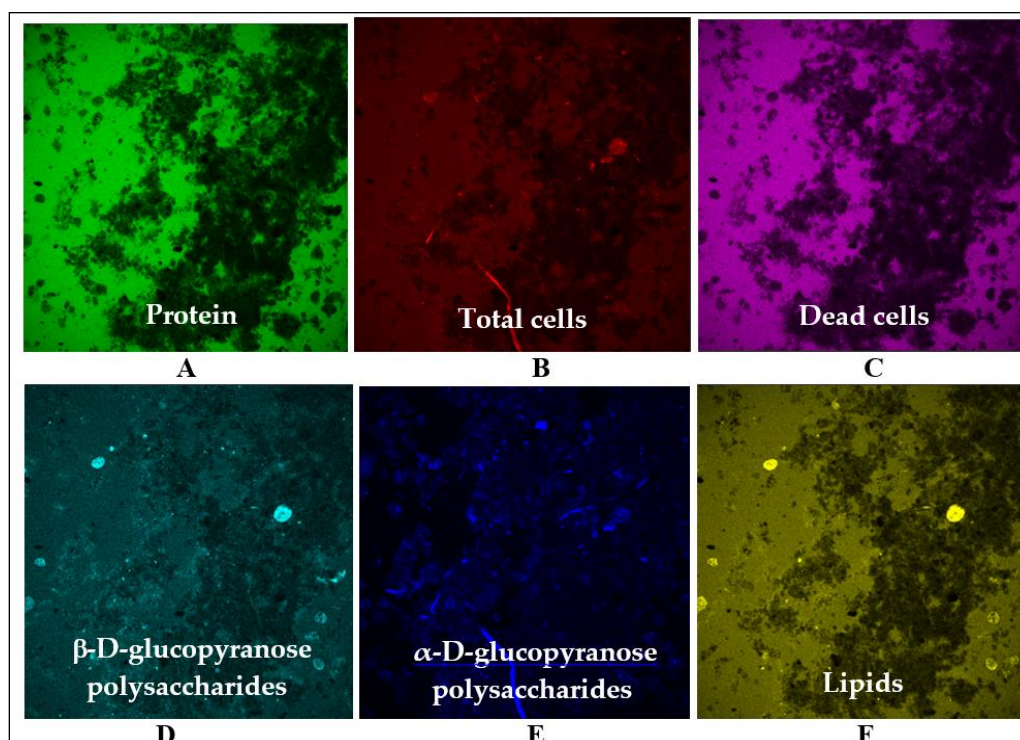


Figure 3: Direct visualization of a stained fouling layer on membrane surface: a) Green (protein), b) Red: (total cells), c) Purple (dead cells), d) Blue (α -D-glucopyranose polysaccharides), e) Light blue (β -D-glucopyranose polysaccharides) and f) Yellow (lipids).

Figure 4 depicts 3D CLSM images captured at various fluorescence intensities and depths within the membrane structure. It should be noted that protein accumulates primarily throughout the membrane structure, reaching a maximum depth of 22 μm (Figure 4A), followed by polysaccharides (Figure 4B). The buildup of these foulants is consistent with the observed decrease in membrane flux of the system. Polysaccharides and proteins, according to Dickinson (Dickinson, 2005) and McClements (McClements, 2006), can form favorable hydrogen bonds or electrostatic interactions.

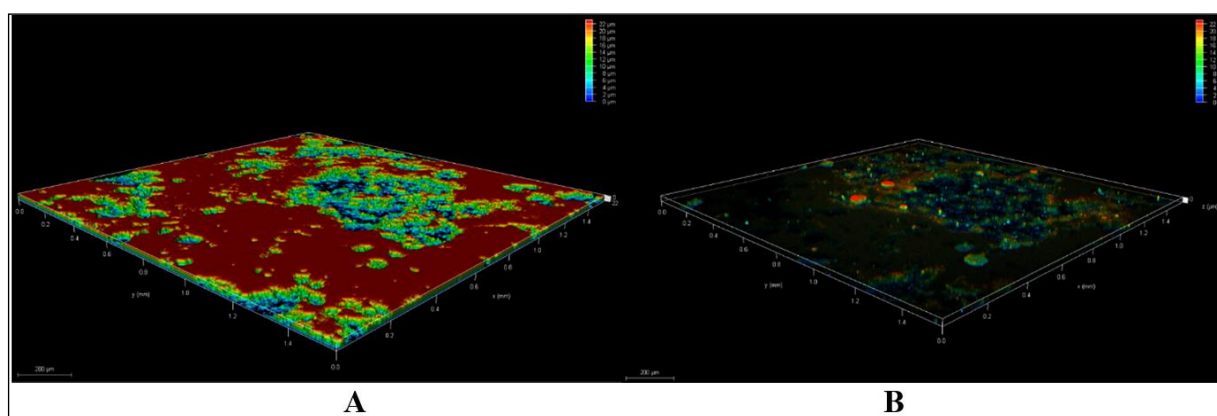


Figure 4: The biofouling 3D CLSM image is further split to denote 3D images of the constituents; (A) Protein, (B) Polysaccharides (Image captured at 10x, scale bar denotes 200 μm , 5 μm below the membrane surface).

3. 3. FESEM-EDX analysis

Foulant morphology was depicted in Figure 5 using FESEM. It should be noted that the membrane pore for a new membrane was clearly visible (Fig. 5a). However, biofouling development had covered the pores over time with various foulants such as microbial flocs and extra polymeric substances (Fig 5b). Bacterial cells (Fig 5c) and other foulants (Fig 5d) have been captured on some parts of the membrane, indicating that microbes have adapted and grown in the MBR system. Membrane flux, according to Cai et al. (2018), influences biofilm development and thus accelerates foulants accumulation. The biofilm significantly reduced the mass transfer coefficient, resulting in marginally reduced water permeability. Bacteria and soluble microbial products clogged the pores of the membrane. As a result of the tortuous paths within the biofilm layer, diffusion of retained solutes was hampered.

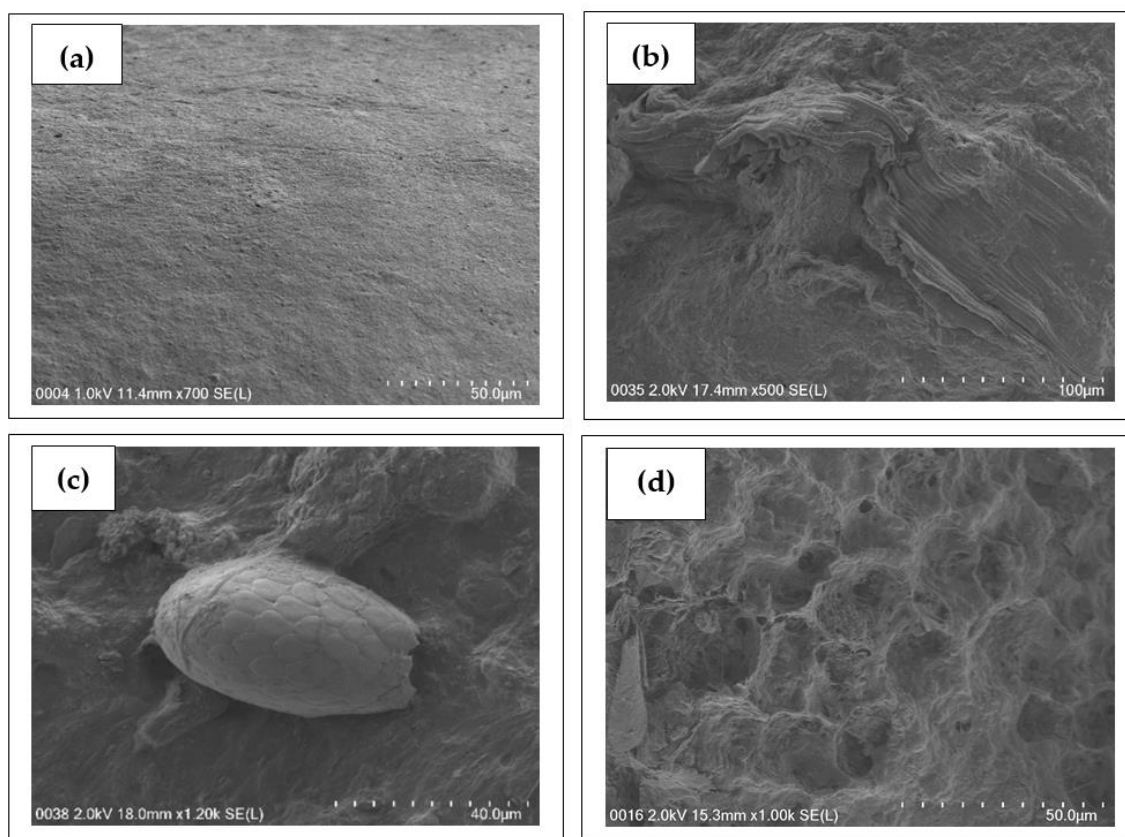


Figure 5: FESEM images: (a) new membrane; (b) fouling bio-cake; (c) bacterial cells; (d) other foulants formed on the membrane surface (at 5000 × magnification).

The elemental composition of the fouled membrane as determined by energy spectrum analysis is shown in Figure 5. The primary constituents of the foulant layer were identified as C, O, Al, and Si peaks. It can be concluded that the cake layer is made up of both organic and inorganic materials that accumulate on the surface of the membrane, which is consistent with the findings of Hu et al. (Hu et al., 2016) and Viet et al. (Viet et al., 2019).

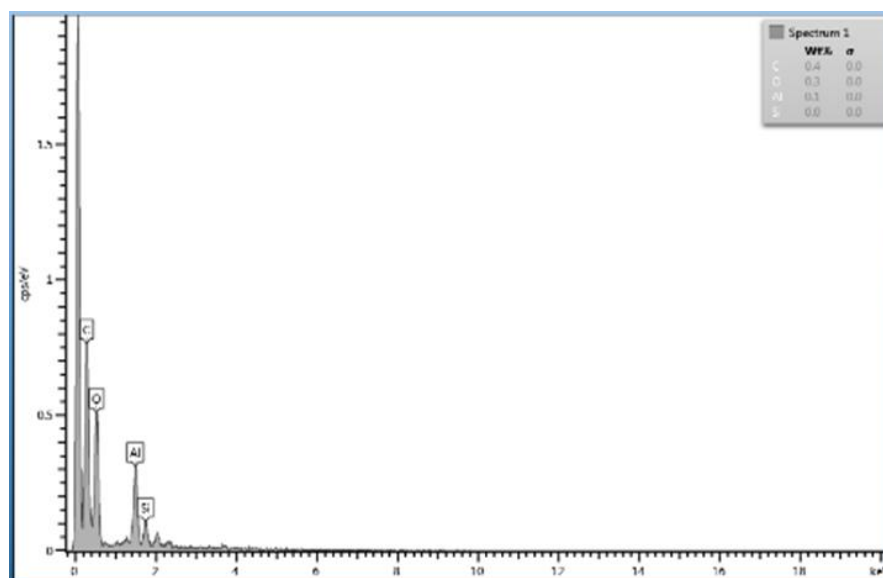


Figure 6: EDX elemental analysis of fouled membrane.

4 Conclusion

The performance of the membrane bioreactor treating actual sewage had shown a remarkable result meeting the effluent discharge standards of Malaysia. The evaluation of fouling layers and the mechanism of biofouling development through profiling of foulant morphology using FESEM and CLSM had been carried out. Pore blocking and cake formation were the dominant foulants in a membrane bioreactor treating actual sewage. In the early stages of the operation, pore-blocking prevails, resulting in a significant decrease in permeation fluxes. Cake formation fouling dominated the majority of the MBR operation and resulted in slower permeation flux decay over time. The fluorescent staining of the fouling layer on the membrane surface revealed that proteins, α -D-glucopyranose polysaccharides, and lipids were aggregated into clusters. FESEM images revealed that the membrane experienced mild internal pore-clogging, implying that fouling occurred mainly on the membrane surface. The biofilm developed only marginally reduced overall water permeability but severely reduced the mass transfer coefficient. As a result, it can be concluded that proteins and microbial cells were the primary constituents of the fouling layer which may have contributed to the membrane performance deterioration after fouling.

Acknowledgments

The authors gratefully acknowledge the support of SEGi University and Indah Water Konsortium (IWK) for the pilot plant study area, which was funded by the Fundamental Research Grant Scheme (FRGS/ 1/ 2019/ TK02/ SEGI/ 02/ 1) under the Ministry of Higher Education of Malaysia (MOHE).

Conflict of interests

The authors declare that there are no competing interests.

References

- Adoonsook, D., Chia-Yuan, C., Wongrueng, A., & Pumas, C. (2019). A simple way to improve a conventional A/O-MBR for high simultaneous carbon and nutrient removal from synthetic municipal wastewater. *PLoS ONE*, *14*(11), 1–27. <https://doi.org/10.1371/journal.pone.0214976>
- Alrhoun, M., Carrion, C., Casellas, M., & Dagot, C. (2014). *Hospital Wastewater Treatment by Membrane Bioreactor: Performance and Impact on the Biomasses*. <https://doi.org/10.15242/iicbe.c0314004>
- APHA. (2005). *Standard Methods for the Examination of Water and Wastewater, 21st Edition*. American Public Health Association (APHA).
- Cai, X., Yu, G., Hong, H., He, Y., Shen, L., & Lin, H. (2018). Impacts of morphology on fouling propensity in a membrane bioreactor based on thermodynamic analyses. *Journal of Colloid and Interface Science*, *531*, 282–290. <https://doi.org/10.1016/j.jcis.2018.07.030>
- Canette, A., & Briandet, R. (2014). Microscopy: Confocal Laser Scanning Microscopy. In *Encyclopedia of Food Microbiology: Second Edition* (Second Edi, Vol. 2). Elsevier. <https://doi.org/10.1016/B978-0-12-384730-0.00214-7>
- Dickinson, E. (2005). *Food Colloids: Interactions, Microstructure and Processing*. Royal Society of Chemistry.
- Du, X., Shi, Y., Jegatheesan, V., & Ul Haq, I. (2020). A review on the mechanism, impacts and control methods of membrane fouling in MBR system. In *Membranes* (Vol. 10, Issue 2). <https://doi.org/10.3390/membranes10020024>
- Fortunato, L., Li, M., Cheng, T., Rehman, Z. U., Heidrich, W., & Leiknes, T. O. (2019). Cake layer characterization in Activated Sludge Membrane Bioreactors: Real-time analysis. *Journal of Membrane Science*, *578*(February), 163–171. <https://doi.org/10.1016/j.memsci.2019.02.026>
- Hu, Y., Wang, X. C., Yu, Z. Z., Ngo, H. H., Sun, Q., & Zhang, Q. (2016). New insight into fouling behavior and foulants accumulation property of cake sludge in a full-scale membrane bioreactor. *Journal of Membrane Science*, *510*, 10–17. <https://doi.org/10.1016/j.memsci.2016.02.058>

- Isik, O., Hudayarizka, R., Abdelrahman, A. M., Ozgun, H., Ersahin, M. E., Demir, I., & Koyuncu, I. (2020). Impact of support material type on performance of dynamic membrane bioreactors treating municipal wastewater. *Journal of Chemical Technology and Biotechnology*, 95(9), 2437–2446. <https://doi.org/10.1002/jctb.6426>
- McClements, D. J. (2006). Non-covalent interactions between proteins and polysaccharides. *Biotechnology Advances*, 24(6), 621–625. <https://doi.org/10.1016/j.biotechadv.2006.07.003>
- Viet, Q., Hu, Y., Li, J., Cho, J., & Hur, J. (2019). Characteristics and influencing factors of organic fouling in forward osmosis operation for wastewater applications: A comprehensive review. *Environment International*, 129(May), 164–184. <https://doi.org/10.1016/j.envint.2019.05.033>
- Yang, Z., Peng, X. F., Chen, M. Y., Lee, D. J., & Lai, J. Y. (2007). Intra-layer flow in fouling layer on membranes. *Journal of Membrane Science*, 287(2), 280–286. <https://doi.org/10.1016/j.memsci.2006.10.051>
- Yang, Y., Zang, Y., Hu, Y., Wang, X. C., & Ngo, H. H. (2020). Upflow anaerobic dynamic membrane bioreactor (AnDMBR) for wastewater treatment at room temperature and short HRTs: Process characteristics and practical applicability. *Chemical Engineering Journal*, 383(August 2019), 123186. <https://doi.org/10.1016/j.cej.2019.123186>